¹ Sabna M

² Mini V P

³Ushakumari S

⁴ Mayadevi N

⁵ Harikumar R

A Single Detection and Diagnosis Algorithm for Electrical Faults in a Five Phase Permanent Magnet Synchronous Motor Drive



Abstract: In all processing and manufacturing industries, approximately half of the operating cost is contributed to the maintenance process. Due to high reliability and fault-tolerant capability, five-phase Permanent Magnet Synchronous Motors (5φ-PMSM) are commonly used in high-power and fault-tolerant applications. Early-stage detection and diagnosis of faults can reduce maintenance costs. This paper proposes a single algorithm for detecting and diagnosing electrical faults such as inter-turn short circuit faults, phase-to-phase faults, phase-to-ground to ground faults, and open circuit faults in a 5φ-PMSM drive. The discrete wavelet transforms, and statistical parameters extract the fault features from the normalized stator currents under normal and faulty conditions. A fuzzy logic system is adopted to diagnose electrical faults and faulty phases. Since the algorithm uses normalized stator currents for fault detection and diagnosis, it can be used for detecting and diagnosing electrical faults in 5φ-PMSM drive with any capacity. The time of fault detection and diagnosis process is less than two cycles of stator current. Finally, the proposed algorithm is experimentally validated using Raspberry Pi.

Keywords: Five phase PMSM, fault detection and diagnosis, short circuit faults, inter-turn short circuit faults, phase to phase faults, phase to ground faults, open circuit faults, electrical faults, discrete wavelet transform, fuzzy logic systems.

I. INTRODUCTION

Fault detection, diagnosis, and protection of electrical machines have a history that is as antiquated as the machines themselves. Recently, research in fault detection and diagnosis of electrical machines has accelerated rapidly. It is essential to detect and diagnose the faults at the initial stage itself to reduce the running cost of an industry. Otherwise, this will lead to an unexpected and unscheduled shutdown of the machine and result in significant financial losses.

In general, faults in PMSM can be categorized into three types based on the nature of the fault: mechanical, magnetic, and electrical. Electrical faults are divided into Short Circuit Faults (SCF) and Open Circuit Faults (OCF). The main types of short circuit faults include Inter Turn Short Circuit Faults (ITSF), Phase to Phase Faults (PPF), and Phase to Ground Faults (PGF). Electrical faults in the stator winding are common in AC machines [1]. This paper focuses on electrical faults and develops a detection and diagnosis algorithm for electrical faults.

Research on fault detection in multiphase PMSM is still in its early stages. In [2], a fault detection technique based on discrete wavelet transform and a diagnosis technique based on a fuzzy logic system for ITSF in a 5ϕ -PMSM is presented. Zhongyi Yang et al. in [3] developed a method to detect ITSF in 5ϕ -PMSM based on Hilbert transform analysis. Even when a single turn is short-circuited, ITSF in 5ϕ -PMSM can be detected using the spectra of stator currents and zero-sequence voltage components, as demonstrated in [4]. For a 5ϕ -PMSM experiencing single-phase SCF and ITSF, the authors in [5] proposed a multi-vector model predictive control with voltage error tracking. A current control technique is reported by Du et al. in [6] to lower the losses of a 5ϕ -PMSM under OCF condition. In [7], a fault-tolerant control technique is proposed for 5ϕ -PMSM with third-order harmonic back EMF under single-phase OCF and SCF. A field-oriented control technique for a 5ϕ -PMSM is suggested by the authors of [8] under OCF conditions. In [9], Chen et al. developed an online diagnosis method based on the magnetic field oscillation for OCF in 5ϕ -PMSM. A fault detection technique based on voltage and fundamental current trajectory distribution features for OCF in a 5ϕ -PMSM is presented in [10]. A short circuit fault detection algorithm for 5ϕ -PMSM drive based on wavelet transform is explained in [11].

Copyright $^{\circ}$ JES 2024 online: journal.esrgroups.org

¹ *Corresponding author: Department of Electrical Engineering, College of Engineering Trivandrum, APJ Abdul Kalam Technological University, Thiruvananthapuram, Kerala, India.

^{2,3,4,5} Department of Electrical Engineering, College of Engineering Trivandrum, APJ Abdul Kalam Technological University, Thiruvananthapuram, Kerala, India.

The literature study revealed that the existing algorithms for fault detection and diagnosis are only capable of identifying a single kind of fault at a time. Consequently, each fault requires a different detection and diagnosis algorithm, which will increase the complexity and cost of the system. To ensure the reliable and uninterrupted operation of motors, a combined fault detection algorithm for a group of faults is essential for a 5ϕ -PMSM drive. This paper proposes a combined detection and diagnosis algorithm for electrical faults in a 5ϕ -PMSM drive, including ITSF, PPF, PGF, and OCF.

This paper is organized as follows: it begins with an introduction. The classification of faults in PMSM is discussed in Section II. In the third section, the analysis of 5ϕ -PMSM drive with various electrical faults is analyzed. Section IV provides a theoretical background of discrete wavelet transforms and fuzzy logic systems. The results and discussion are explained in the fifth section, followed by experimental validation. The last section includes the conclusion and discusses the future scope of the work.

The key contributions of this paper are as follows:

- Developed a model of 5ϕ -PMSM drive and electrical faults using the external editor platform of Ansys software.
- Analyzed the performance of the developed motor.
- The fault feature is extracted using the wavelet transform and mathematical parameters.
- Developed a single fault detection and diagnosis algorithm for all electrical faults, including ITSF, PPF, PGF, and OCF, using a knowledge-based fuzzy logic system for 5ϕ -PMSM drive with any capacity.
- The fault detection and diagnosis time is less than two cycles of stator current.

II. CLASSIFICATION OF FAULTS IN PMSM

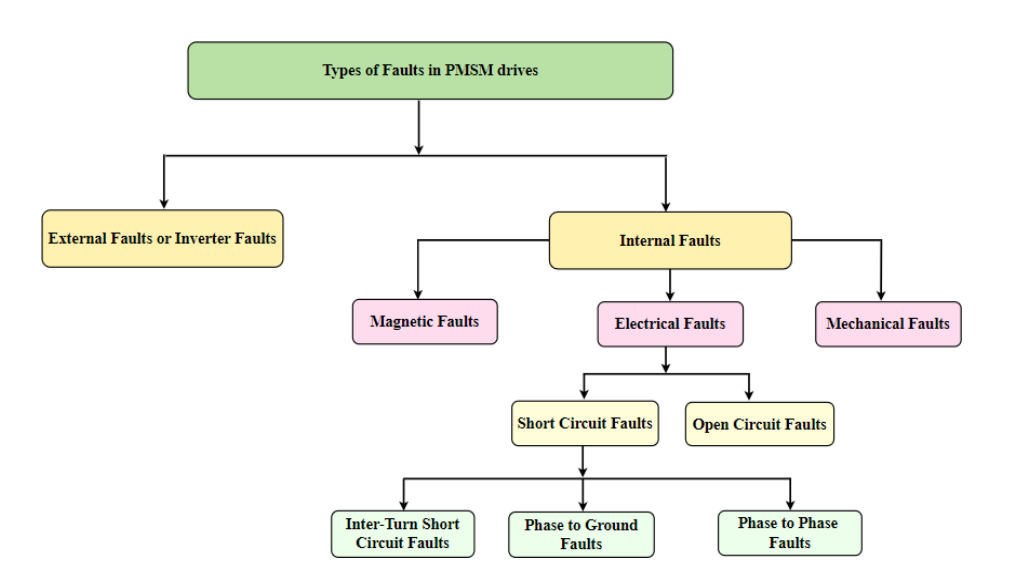


Fig. 1 Classification of faults in $5\phi\text{-PMSM}$ drive

In PMSM, the faults are mainly categorized into mechanical faults, electrical faults, magnetic faults and as shown in Fig. 1. Mechanical faults are related to the air gap, bearings, and alignment in the stator and rotor, whereas electrical faults are related to the windings in the stator. The magnetic fault is associated with the permanent magnet rotor. The present status of different faults occurring in PMSM is 41% faults are bearing related, 37% faults are stator related, 10% faults are rotor related and the remaining 12% are other faults [1].

2.1 Electrical Faults

The electrical faults are due to either short circuits or open circuits of windings in the stator part of the motor. Insulation failure, overheating, or overload are the primary reasons for electrical faults. The most frequent electrical fault in PMSM is ITSF in the stator windings. This fault generates a significant amount of heat and circulating current in the shorted path, making it particularly challenging. If not identified and removed promptly, it can spread into more stator windings and produce PPF, PGF, and even demagnetization faults [12]. An OCF in a PMSM typically occurs when a phase winding is disconnected from the power source. This disconnection may result from either an internal failure of the stator winding or a mechanical failure of the terminal connector. Such faults lead to significant electromagnetic torque ripples, considerable mechanical vibrations, and notable fluctuations in motor performance, including variations in speed and torque, as well as unbalanced currents in the stator winding. Consequently, these issues generate excessive heat within the winding.

2.2 Mechanical Faults

The mechanical faults include shaft bending, bolt loosening, bearing issues, and air gap eccentricity. Among these, bearing faults are the most common mechanical faults, and the main causes of these faults are vibrations, shaft misalignment, inadequate lubrication, overload, and corrosion [13]. Even during regular operation, bearings are subject to wear and tear. Bearing degradation can cause mechanical faults such as air gap eccentricity, and increased friction.

2.3 Magnetic Faults

PMSM can be demagnetized by various factors, such as high temperature, large short-circuit currents, damage to the magnet, armature reaction, and aging of the magnet itself [14]. When a demagnetization fault occurs, it can cause ripples in flux linkage which lead to insufficient torque. To compensate for this, the motor needs more current to provide the necessary torque, which in turn raises the temperature and worsens the demagnetization. This fluctuation in torque can also produce abnormal vibration and acoustic noise. In addition, this torque variation can lower the performance and efficiency of the motor. Of all the faults listed above, electrical faults are the most serious and frequent ones, and if not detected in time, this may lead to other faults like magnetic and mechanical faults. So, it is necessary to detect and diagnose the electrical faults at the initial stage itself and the authors proposed a single algorithm to detect and diagnose these faults.

III. PERFORMANCE ANALYSIS OF 5ϕ -PMSM DRIVE

A 220V, 50Hz, 1500rpm, 1kW 5ϕ -PMSM drive is selected, and the detailed design procedures are explained in [15]. The dimensions obtained are presented in Table 1. A 5ϕ -PMSM drive with these dimensions was developed using Ansys software, and its 2D model is depicted in Fig. 2. The analysis of the developed model is done. Fig.3 shows the stator current with a peak value of 2.06A under full load and healthy conditions. Fig. 4 and Fig. 5 illustrate the torque and speed of the motor under healthy conditions. The motor attains a rated speed of 1500 rpm with a rated torque of 6.5 Nm at 100ms.

The electrical faults such as ITSF, PPF, PGF, and OCF are created in the 5ϕ -PMSM model using the external editor platform of Ansys software and analyzed its characteristics under various fault conditions. The fault was introduced at t=0.15 sec. The performance of the motor under different electrical faults, including ITSF, PPF, PGF, and OCF will be illustrated in the following section.

Table 1 Designed values

Parameter	Quantity
D	113 mm
L	97 mm
L_{PM}	5 mm
h_S	13 mm
S	40
Tp	184
Z	1870

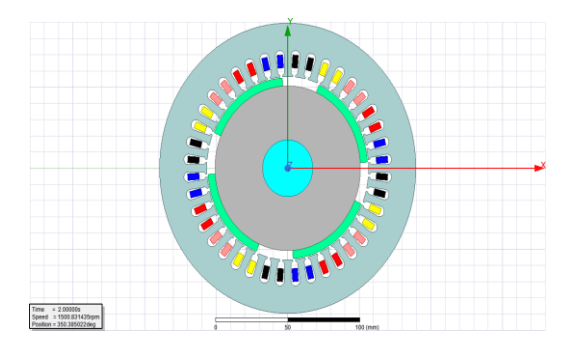


Fig. 2 Developed model of 5φ-PMSM drive

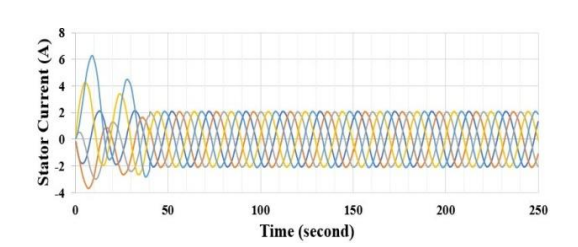


Fig. 3 Full load current response of healthy motor

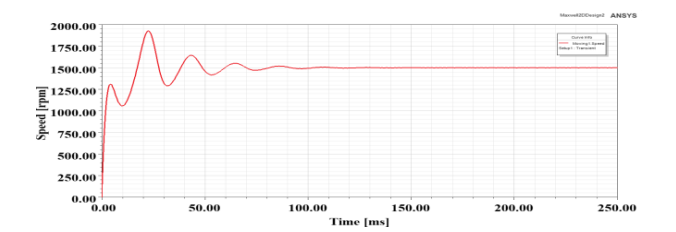


Fig. 4 Speed response of healthy motor

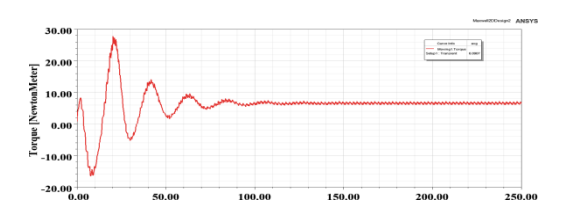


Fig. 5 Torque of healthy motor

3.1 Inter-Turn Short Circuit Fault Analysis

An ITSF is developed in the stator winding of the 5ϕ - PMSM drive, by connecting a very low value of resistance (R_f) in parallel with some portions of the stator winding using the external circuit editor platform of Ansys Maxwell software. Fig. 6 depicts the equivalent stator winding of 5ϕ -PMSM drives with ITSF in "phase A". The fault is introduced at t=0.15 sec, and the performance analysis of the developed motor with ITSF is carried out. The stator current of "phase A" winding with ITSF is shown in Fig. 7, where the magnitude of currents in phase "A" increased rapidly after the occurrence of a fault, and all other phase currents become distorted.

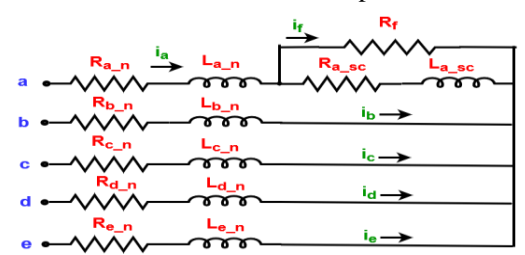


Fig. 6 Stator winding with ITSF in phase A

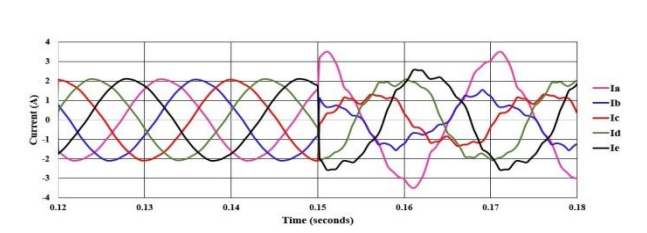


Fig. 7 Full load current response of ITSF in phase A

The analysis is done with ITSF in different phases, and the resulting stator currents are depicted in Fig. 8. The magnitude of the current in the faulty phase becomes increased and distorted, and the other stator currents are also distorted, and detailed analysis is explained in [16].

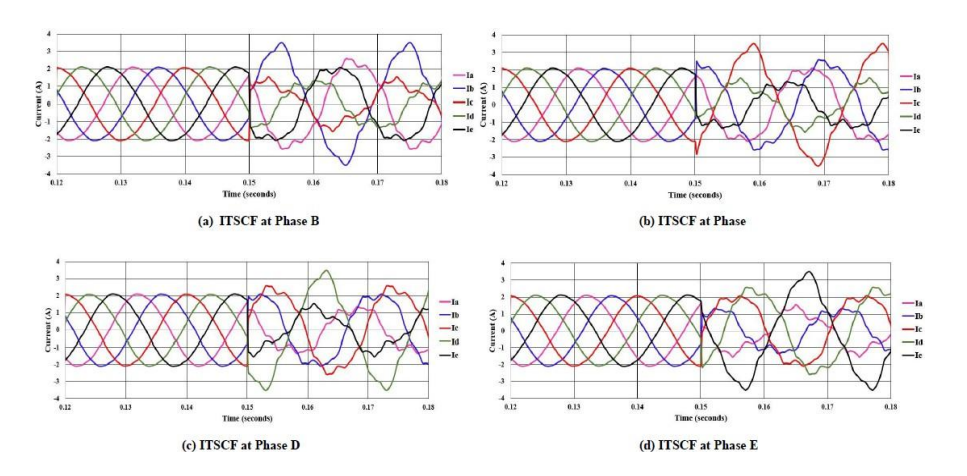
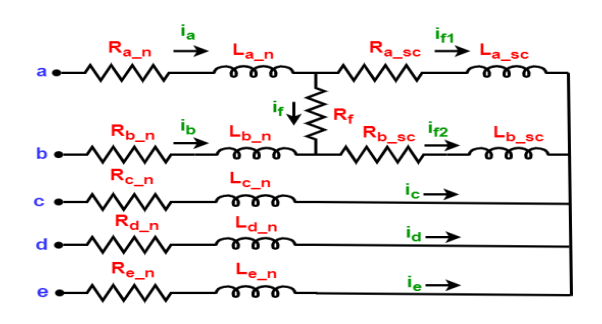


Fig. 8 Full load current response of the motor under ITSF in different phases

3.2 Phase to Phase Fault Analysis

A PPF is developed in the stator winding of the 5ϕ - PMSM drive, by connecting a very low value of resistance ($R_{\rm f}$) between two phases of the stator winding using the external circuit editor platform of Ansys software. An equivalent stator circuit of 5ϕ -PMSM drives with PPF is illustrated in Fig. 9, where the fault is developed between "phase A and B". The fault is created at t=0.15 sec, and the analysis of the motor with PPF is carried out. The stator current waveforms with PPF between "phase A and B" conditions are shown in Fig. 10, where the magnitude of currents in "phase A and B" increased rapidly after the occurrence of a fault, and all other phase currents become distorted.



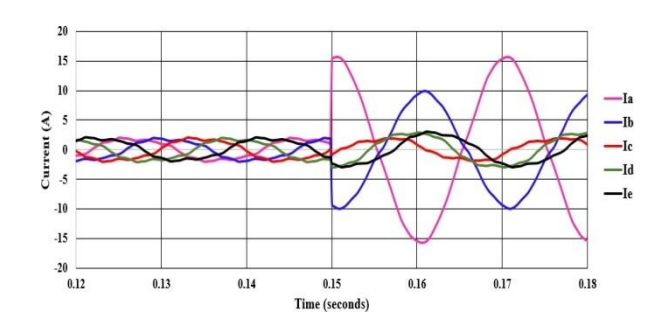


Fig. 9 Stator windings with PPF in phases A and B

Fig. 10 Full load current response of PPF in phases A and B

The analysis is done with PPF occurring in different phases, and the resulting stator current response is depicted in Fig. 11 and Fig. 12. It is observed that the stator current in the faulty phases becomes distorted and increased, and other stator currents become distorted. The schematic diagram of the stator winding of 5ϕ - PMSM drive with PGF at "E phase" is depicted in Fig. 13. The PGF is developed in the stator winding, by connecting a very low value of resistance (R_f) in between stator winding and the ground using the external circuit editor platform of Ansys software.

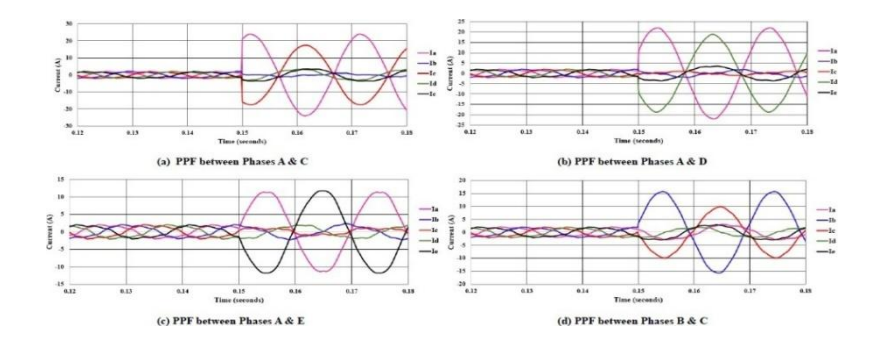


Fig. 11 Full load current response of PPF between different phases

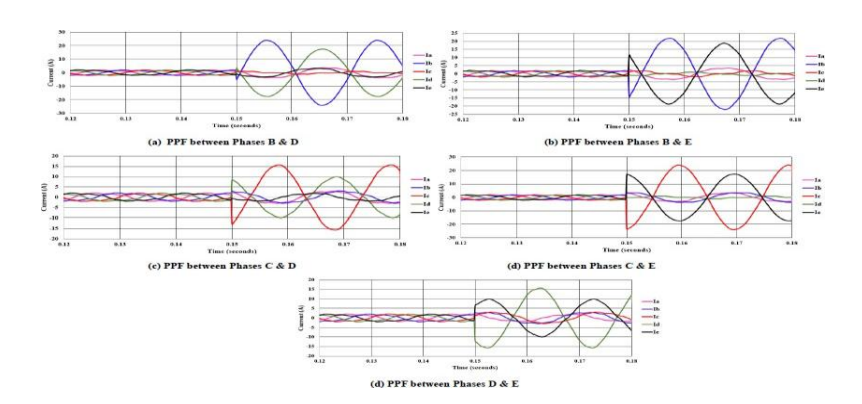


Fig. 12 Full load current response of PPF between different phases

3.3 Phase to Ground Fault Analysis

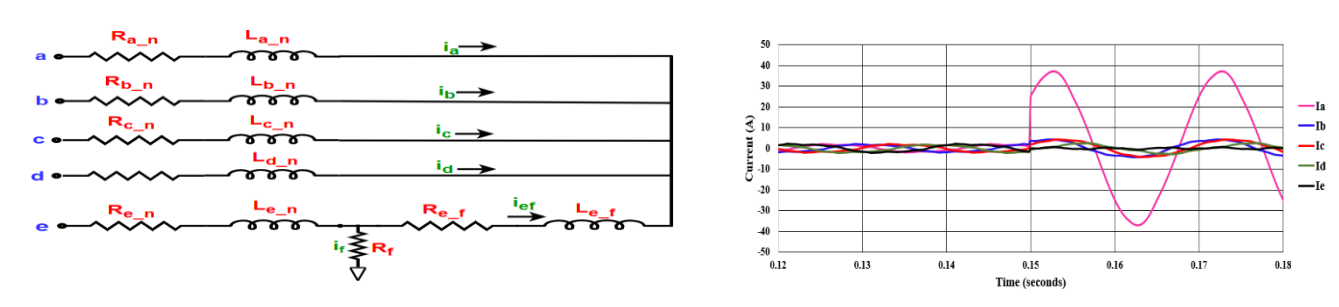


Fig. 13 Stator windings with PGF in phase E

Fig. 14 Full load current response of PGF phase E $\,$

The fault is created at t=0.15 sec, between "phase E and ground", and the corresponding stator currents are depicted in Fig. 14. In the faulty phase, the current suddenly rises to a high value, and the currents in the other phases are also changed.

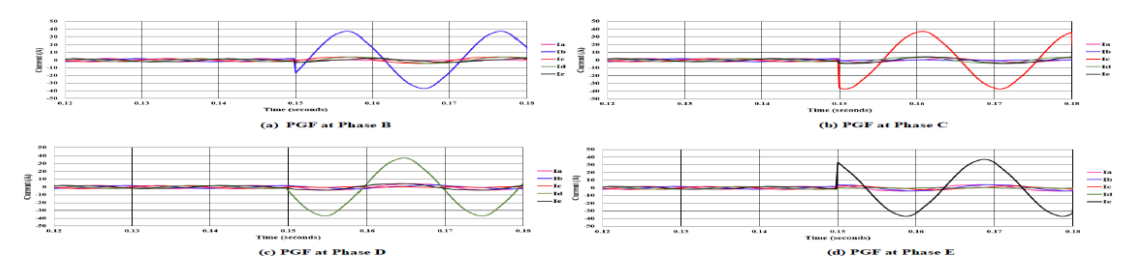
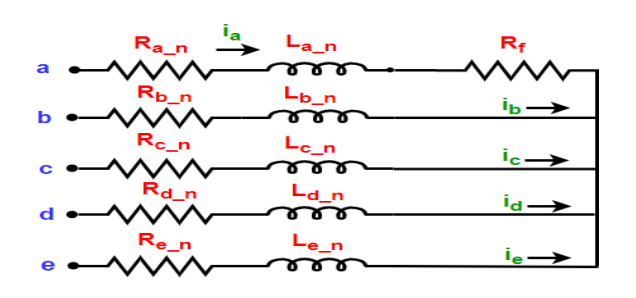


Fig. 15 Full load current response of PGF in phases A, B, C, and D

The analysis is done with PGF at different phases, and the resulting stator current response is depicted in Fig. 15. It is observed that the stator current in the faulty phase becomes distorted and increased, and the other stator currents exhibit distortion.

3.3 Open Circuit Fault Analysis



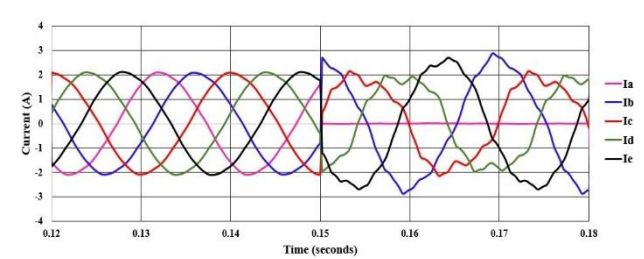
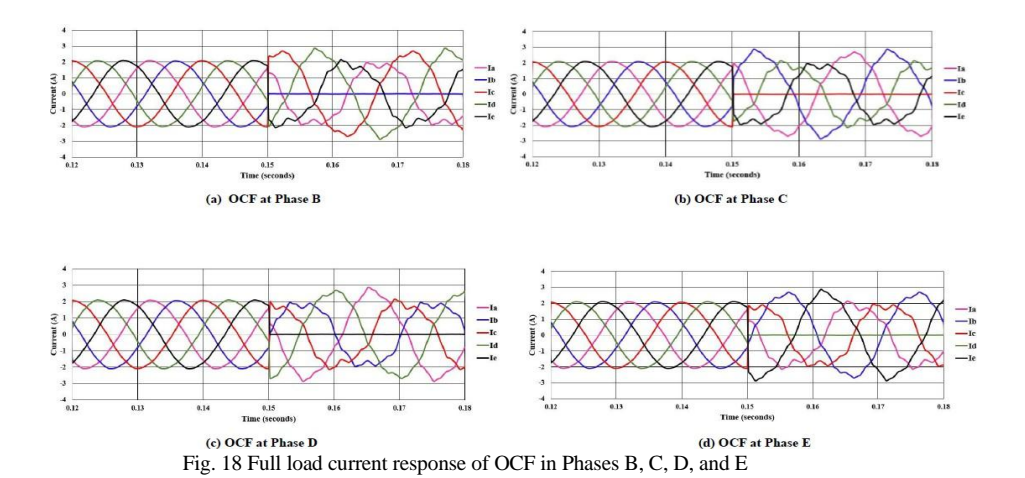


Fig. 16 Stator windings with OCF in phase A

Fig. 17 Full load current response of OCF in phase A

An OCF is developed in 5ϕ - PMSM drive by connecting a very high-value of resistance (R_f) in series with the stator winding using an external circuit editor platform of the Ansys software. An equivalent diagram of the stator winding of 5ϕ - PMSM drive with OCF in "phase A" is shown in Fig. 16.

The fault is introduced at t = 0.15 sec, and the performance analysis of the developed motor with OCF at "phase A" is carried out. The corresponding stator currents are shown in Fig. 17 and is seen that the current in "phase A" drops to zero, and the other phase currents become distorted and changed. The analysis of 5ϕ -PMSM drive with OCF at different



phases is carried out, and the corresponding stator currents are depicted in Fig. 18. The current in the winding experiencing OCF drops to zero, and the currents in the other phases become distorted and increased.

The analysis of 5ϕ -PMSM drive with all the electrical faults such as ITSF, PPF, PGF, and OCF are done. The current under normal and different electrical fault conditions are considered for further process.

IV. DETECTION AND DIAGNOSIS PROCESS

The general block diagram for the fault detection and diagnosis process is shown in Fig. 19. The current signals from the 5ϕ -PMSM drive are fed to the signal processing unit through a signal acquisition unit. In this unit, these signals are processed with different signal-processing techniques Then the processed signals are analyzed to extract the fault-indicating parameters to detect the faults using various statistical parameters. The final stage of the process is to diagnose the faults using either signal-based, model-based, or knowledge-based methods.

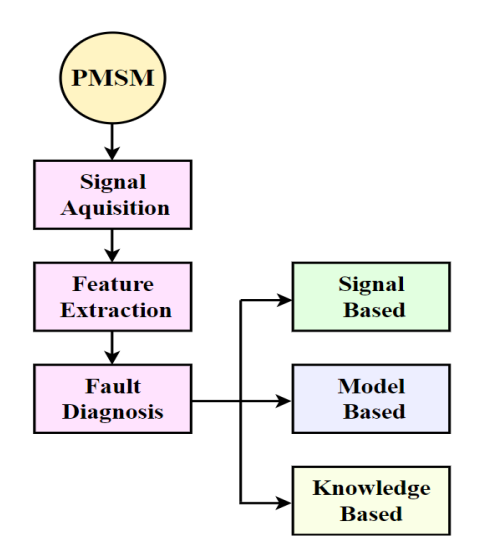


Fig. 19 Block diagram of fault detection and diagnoses process

For evaluating the nonstationary signals, Short Time Fourier Transform (STFT) and wavelet analysis are commonly used methods. STFT uses a window function with a predetermined length and type to split the non-stationary signal into stationary segments. Each segment is then assumed as stationary and the Fast Fourier Transform (FFT) of stationary segments is carried out. The wavelet analysis has been developed to overcome the limitations of STFT and has become one of the most prominent techniques.

In wavelet analysis, the signal is divided into small oscillations of specific time and frequency. The primary benefit is that it offers good time resolution at high frequencies and good frequency resolution at low frequencies. Among the wavelet analysis types, even though both methods yield equally accurate results, a Discrete Wavelet Transform (DWT) is more effective since it requires less data for processing than Continuous Wavelet Transforms (CWT). In this paper, the DWT is used for the analysis process. In the DWT algorithm, the input signal, y(n) is divided into various frequency bands using Low Pass Filters (LPF) and High Pass Filters (HPF) to obtain the approximation constants (Yac) and the detailed constants (Ydc) [17]. The outputs from the LPF are down-sampled by a factor of 2 to obtain coefficients at various levels, and the process is repeated up to the nth level. A block diagram of this decomposition process in multiresolution DWT is shown in Fig. 20.

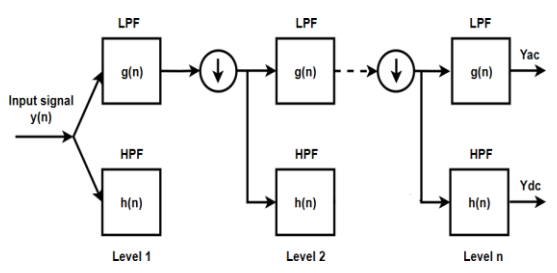


Fig. 20 Decomposition process of Wavelet Transform

To handle a vast amount of data, artificial intelligence (AI), is the best method for fault detection and identification of electrical machines. One of the simplest and most accurate AI for decision-making tasks is fuzzy logic systems [18]. The traditional model of a fuzzy logic system is illustrated in Fig. 21.

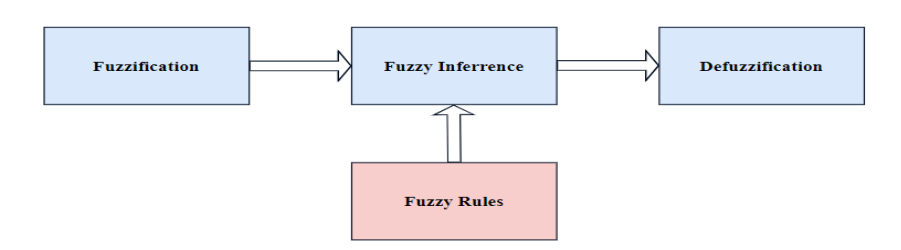
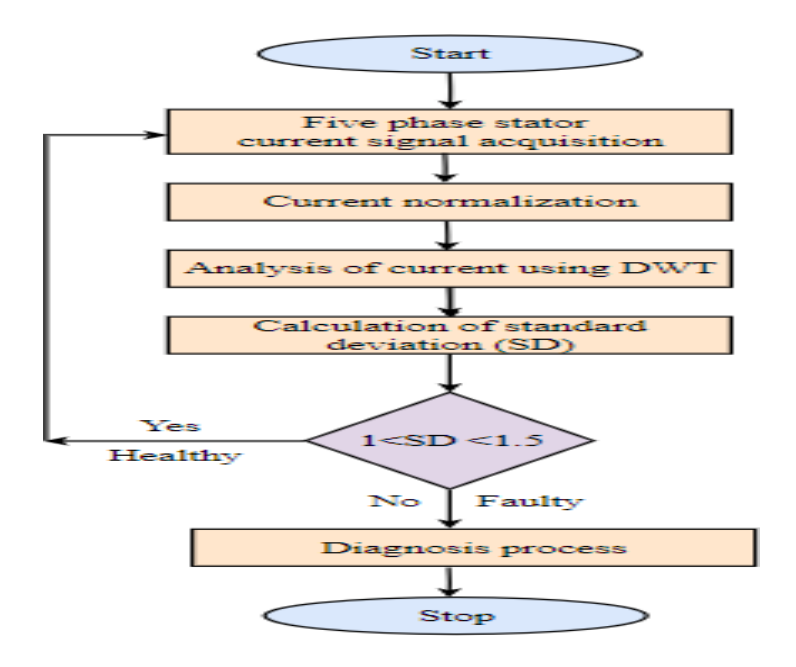


Fig. 21 Block diagram for Fuzzy Logic System

There are three main processes between the input and the output: fuzzification, fuzzy inference, and defuzzification. During the fuzzification process, crisp input data is converted into fuzzy sets using input membership functions. Commonly used membership functions include Gaussian, trapezoidal, and triangular shapes. The fuzzified data is then fed into the fuzzy inference system. This system employs "if-then" rules, utilizing logical operators like "and" and "or" to establish the relationships between the input fuzzy data and the output fuzzy data. The decisions are made based on these fundamental rules. In the defuzzification process, the output membership function is used to convert fuzzy sets back into actual values.

V. RESULTS AND DISCUSSION

The flowchart for the detection and diagnosis algorithm is illustrated in Fig. 22. The electrical faults including ITSF, PPF, PGF, and OCF are developed in the 5ϕ -PMSM drive using the external editor platform of Ansys Maxwell software, and the performance characteristics are analyzed. For fault feature extraction, two cycles of normalized stator currents are analyzed continuously with DWT. In this work, Daubechies 1 (Db 1) mother wavelet and the 4th level of the detailed coefficients are selected because these values exhibit a significant change between the healthy and faulty conditions. The normalized stator current of 5ϕ -PMSM drives under healthy conditions, and the corresponding wavelet window is shown in Fig. 23 and Fig. 24.



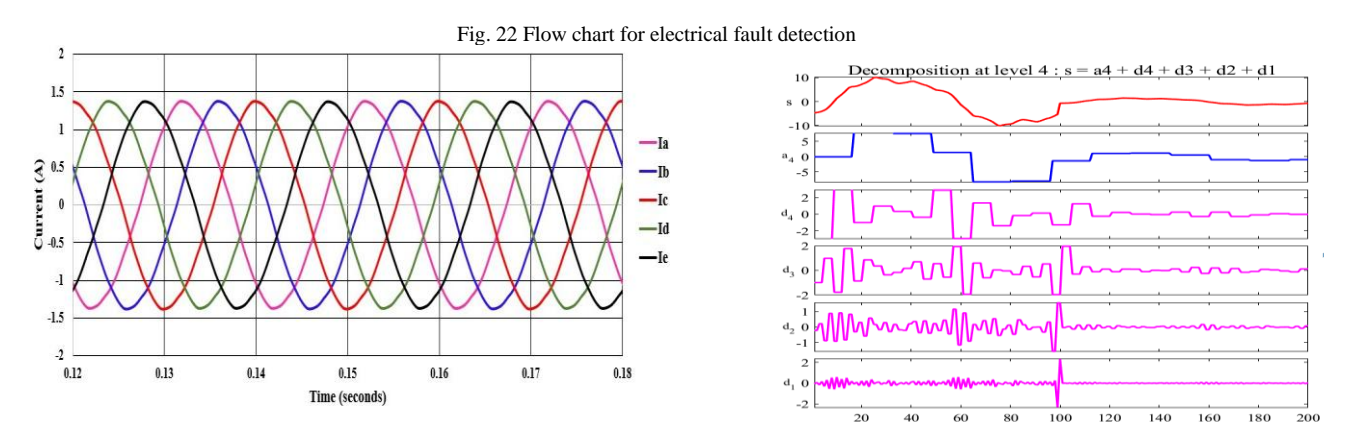
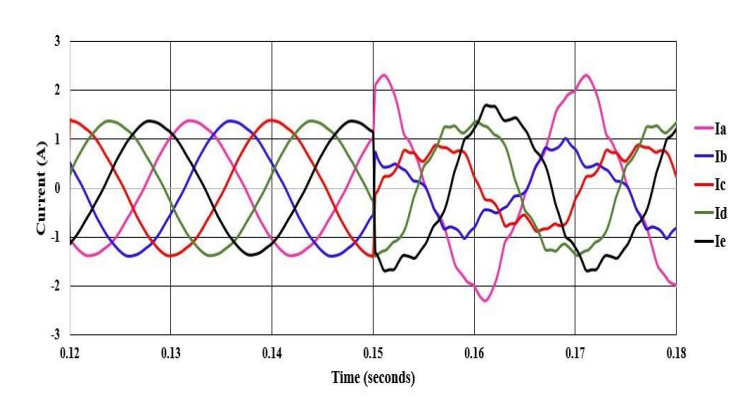


Fig. 23 Normalized stator current under healthy condition

Fig. 24 Wavelet window for healthy condition

In Fig. 24, the top signal represents the original signal, and the second signal displays the approximation coefficient signal at level four. The remaining signals are the detailed coefficient signals from levels 1 to 4.

The normalized stator current and wavelet window of 5ϕ -PMSM drives under different electrical fault conditions (such as ITSF, PPF PGF, and OCF) are shown in Fig. 25 to Fig. 32.



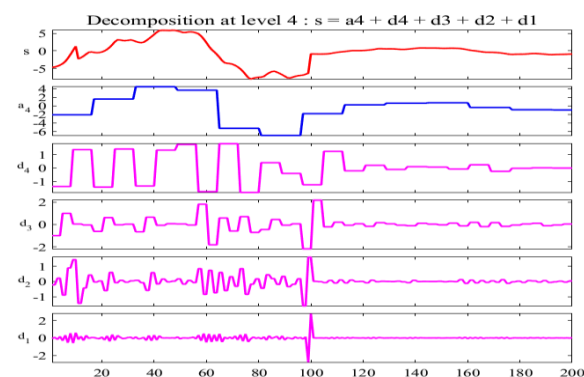
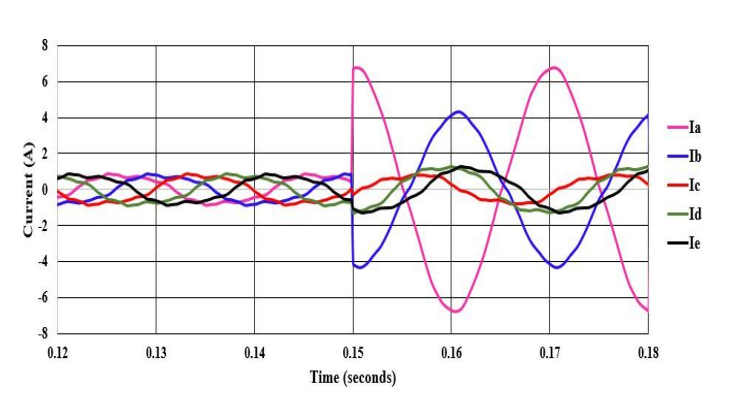


Fig. 25 Normalized stator current under ITSF at phase A

Fig. 26 Wavelet window for ITSF at phase A



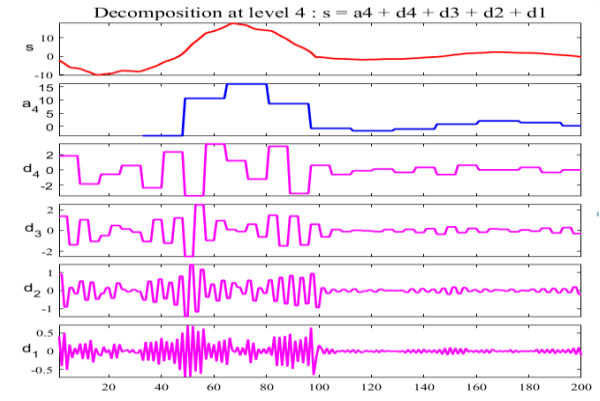
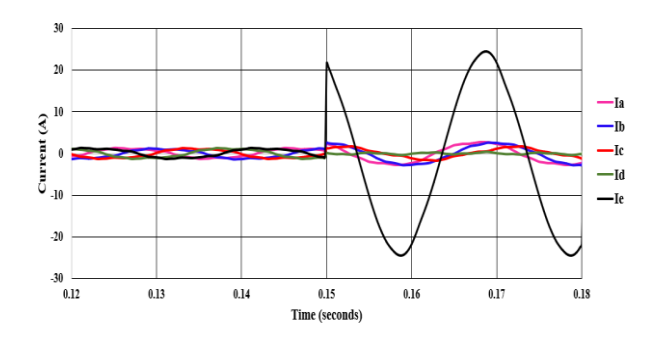


Fig. 27 Normalized current under PPF between A & B

Fig. 28 Wavelet window for PPF between A&B



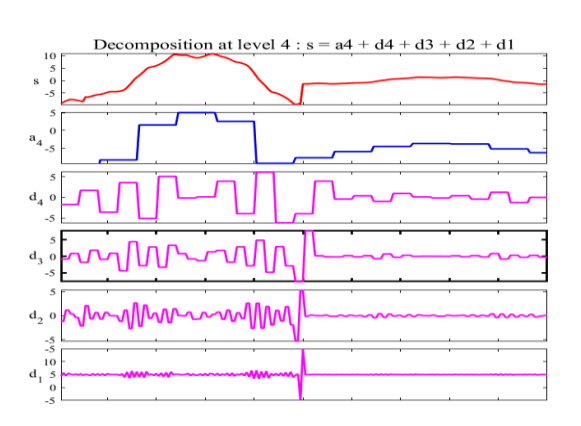
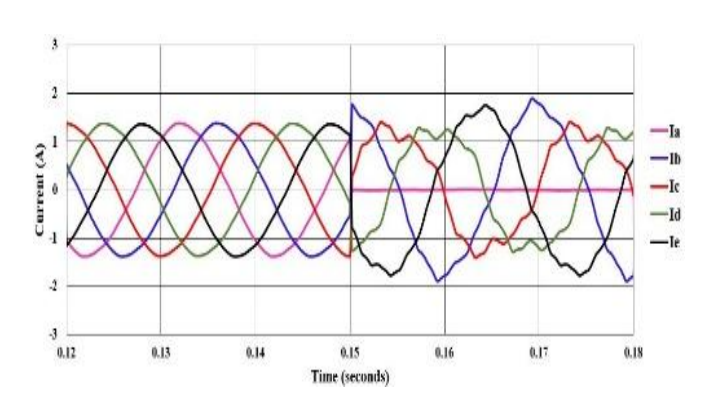


Fig. 29 Normalized stator current under PGF at phase E

Fig. 30 Wavelet window for PGF at phase E

In this work, the detailed coefficients of the fourth level of the Db1 mother wavelet are chosen. The standard deviation (SD) of these coefficients for two cycles of normalized stator currents under healthy and different electrical fault circumstances has been computed and is presented in Table 2. Under normal operating conditions, the SD values presented in Table 2 fall within the range of 1 to 1.5. These SD values deviate from this range, either below 1 or above 1.5 when a fault occurs. This deviation serves as the basis for identifying a fault, enabling the development of a detection

algorithm. Table 2 reveals some uncertainty or ambiguity in the SD values of stator current under healthy and various fault conditions. A fuzzy logic system is used to address this uncertainty and diagnose the faults.



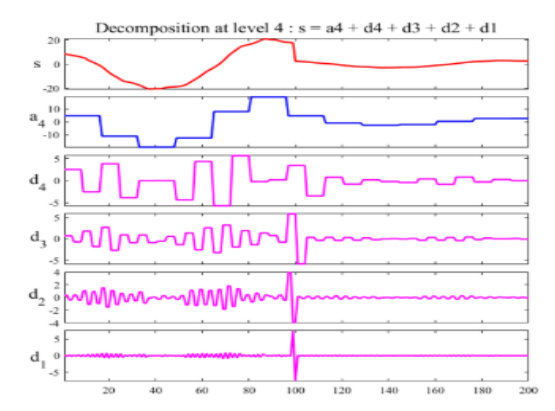


Fig. 31 Normalized stator current under OCF at phase A

Fig. 32 Wavelet window for OCF at phase A

These SDs of 4th level of the Ydc of Db1 wavelets of normalized currents under both healthy and various electrical fault states serve as the input of the diagnosis algorithm. In this fuzzy logic-based diagnosis system, trapezoidal membership functions are used as input functions. The input membership function (range from 0 to 30) includes nine variables, namely Extreme Small (ES), Very Very Small (VVS), Very Small (VS), Small (S), Medium (M), Very Medium (VM), Large (L), Very Large (VL), and Very Very Large (VVL) and shown in Fig. 33. The output membership function also uses trapezoidal membership functions and ranges from 0 to 52 and is shown in Fig. 34. For the diagnosis purpose of each fault, this output membership is divided into five sections: normal case (N) from 0 to 2, ITSF from 2 to 12, PPF from 12 to 32, PGF from 32 to 42, and OCF from 42 to 52 and are shown in Fig. 35 to Fig. 38 respectively.

Table 2 SD-detailed coefficients-electrical faults

SL No	Type of fault	SD (Ia)	SD (Ib)	SD (Ic)	SD (Id)	SD (Ie)
1	HEALTHY	1.339	1.476	1.405	1.185	1.026
2	ITSF A	2.158	1.501	1.04	1.369	1.369
3	ITSF B	1.75	2.186	1.089	1.023	1.137
4	ITSF C	1.529	1.832	2.258	1.204	0.8798
5	ITSF D	1.08	1.711	1.644	1.721	0.842
6	ITSF E	1.368	1.539	1.438	1.551	2.439
7	PPF AB	11.51	8.574	1.285	1.77	1.627
8	PPF AC	16.48	1.651	12.57	1.995	2.096
9	PPF AD	12.3	1.566	0.87	10.41	1.901
10	PPF AE	6.115	1.554	0.9835	1.087	6.381
11	PPF BC	1.981	8.344	5.14	1.162	1.55
12	PPF BD	2.396	14.17	1.022	10.49	1.719
13	PPF BE	2.459	16.11	1.357	0.9304	13.05
14	PPF CD	2.056	2.014	11.88	8.588	1.143
15	PPF CE	2.277	2.485	19.28	1.363	14.84
16	PPF DE	1.348	2.072	1.847	10.03	7.019
17	PGF A	23.08	2.658	2.529	1.791	0.9932

18	PGF B	1.116	24.5	2.571	2.47	1.635
19	PGF C	2.058	1.98	29	2.711	2.488
20	PGF D	2.619	1.679	0.8097	19.63	2.198
21	PGF E	2.893	2.788	1.913	1.367	28.72
22	OCF A	0.8201	1.773	1.252	1.202	1.379
23	OCF B	1.508	0.9249	1.993	1.647	1.168
24	OCF C	1.798	1.452	0.498	1.219	1.049
25	OCF D	1.564	1.762	1.818	0.8257	1.514
26	OCF E	1.823	1.389	1.738	1.54	0.4214

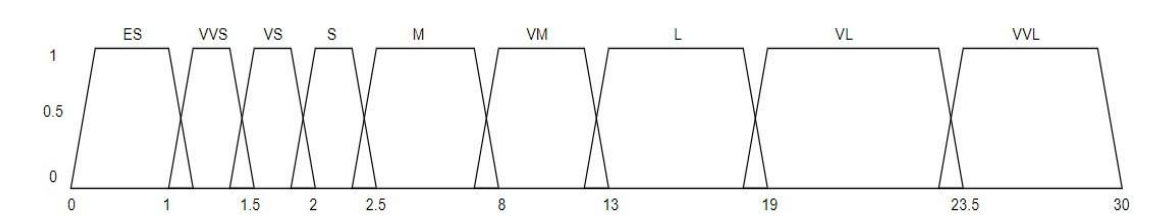
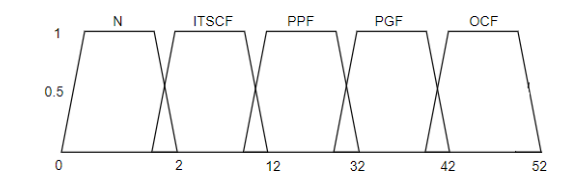


Fig. 33 Input membership function



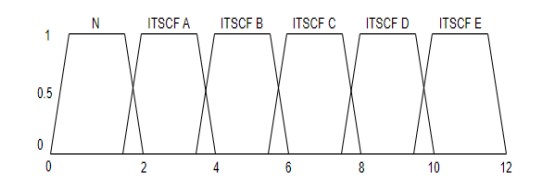
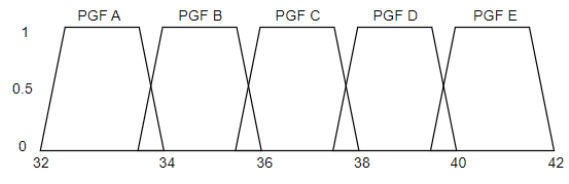


Fig. 34 Output membership function

Fig. 35 Output membership function for ITSF



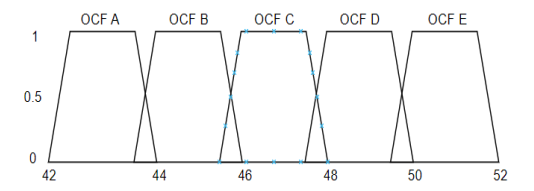


Fig. 36 Output membership function for PGF

Fig. 37 Output membership function for OCF

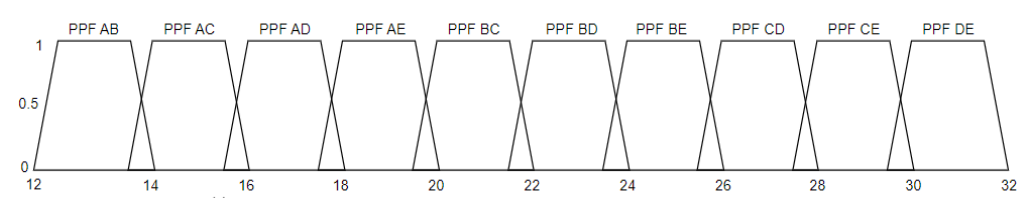


Fig. 38 Output membership function for PPF

The range of output membership function values under normal, ITSF, PPF, PGF, and OCF conditions are given in Table 3. The center of the average approach is used for the defuzzification process. The fuzzy rules are developed in the fuzzy inference system with input to the system and the input membership function, and some of the rules are listed in Table 4.

In this fault diagnosis algorithm, the results are presented in the rule viewer window of the fuzzy logic system. Fig. 39 shows the rule viewer window of the system under normal conditions and shows that the displayed value is 1.1, which is within the range of healthy conditions (0 to 2). Fig. 40 presents the rule viewer window of an ITSF that occurred in the C phase, with a displayed value of 7. This value lies between 6 and 8, fitting within the limits of the output membership function for ITSF in the C phase. Fig. 41 depicts the rule viewer window of PPF that occurred between phase A and phase B, with a displayed value of 13. This value lies between 12 and 14, fitting within the limits of the output membership function for PPF between phase A and phase B. The rule viewer window of PGF at phase D is shown in Fig. 42, with a displayed value of 38.9. This value falls within the range of 38 to 40, which is the output membership function indicating PGF at phase D. Also, Fig. 43 represents the rule viewer window of OCF at phase B, showing a displayed value of 45.1. This value is also within the acceptable limit of the output membership function for OCF at phase B.

Table 3 Range of outputs of fuzzy system

Sl No	Type of fault	Range	Sl No	Type of fault	Range
1	Healthy	0 to 2	14	PPF CD	26 to 28
2	ITSCF A	2 to 4	15	PPF CE	28 to 30
3	ITSCF B	4 to 6	16	PPF DE	30 to 32
4	ITSCF C	6 to 8	17	PGF A	32 to 34
5	ITSCF D	8 to 10	18	PGF B	34 to 36
6	ITSCF E	10 to 12	19	PGF C	36 to 38
7	PPF AB	12 to 14	20	PGF D	38 to 40
8	PPF AC	14 to 16	21	PGF E	40 to 42
9	PPF AD	16 to 18	22	OCF A	42 to 44
10	PPF AE	18 to 20	23	OCF B	44 to 46
11	PPF BC	20 to 22	24	OCF C	46 to 48
12	PPF BD	22 to 24	25	OCF D	48 to 50
13	PPF BE	24 to 26	26	OCF E	50 to 52

Table 4 Fuzzy rules for healthy and faulty conditions

SL						Condition of
NO	Ia	Ib	Ic	Id	Ie	the motor
1	VVS	VVS	VVS	VVS	VVS	
2	VS	VS	VS	VVS	VVS	HEALTHY
3	S	VS	VVS	VVS	VVS	ITSCF A
4	S	VS	VVS	VS	VS	HSCI A
5	VS	S	VVS	VVS	VVS	ITSCF B
6	VS	VM	M	VVS	VS	PPF BC

7	S	S	VM	VM	VVS	PPF CD	
8	VL	M	M	VS	ES	۸G	
9	VVL	M	M	VS	VVS	AG	
10	VVS	VL	M	S	VS	BG	
11	VVS	VVL	M	S	VS	DU	
12	VS	VS	VS	ES	VS	DOC	
13	VS	VS	S	ES	VS	DOC	
14	VS	VVS	VS	VS	ES	EOC	
15	S	VS	VS	VS	ES	EOC	

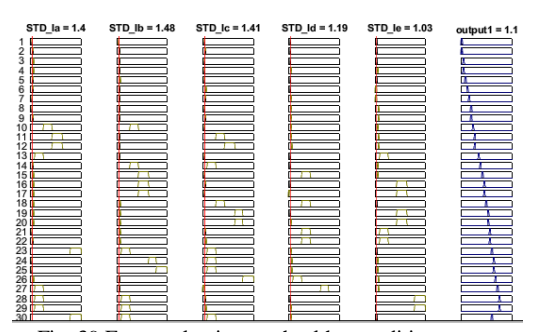


Fig. 39 Fuzzy rule viewer - healthy condition

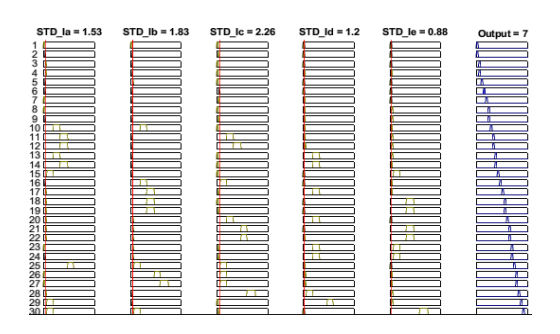


Fig. 40 Fuzzy rule viewer - ITSC at C phase

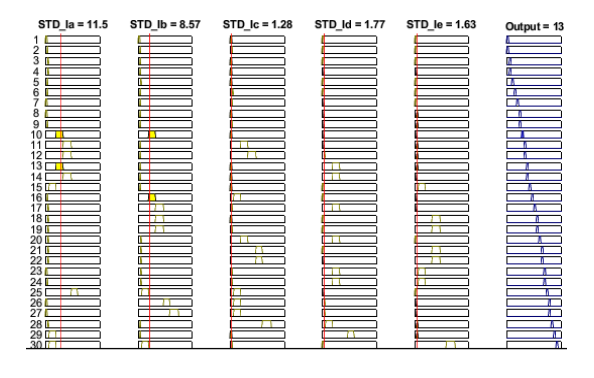


Fig. 41 Fuzzy rule viewer - PPF between A & B phases

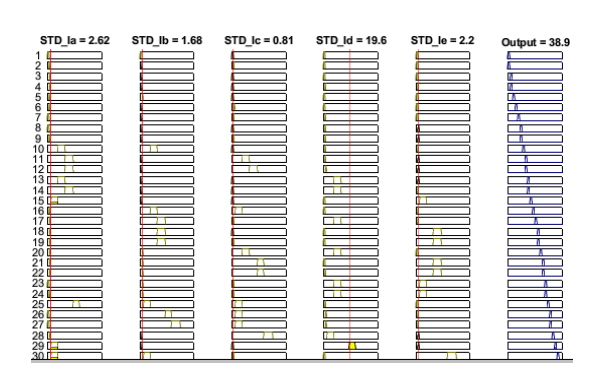


Fig. 42 Fuzzy rule viewer - PGF at D phase $\,$

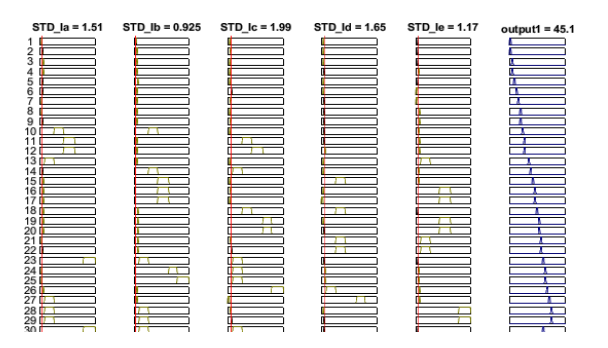


Fig. 43 Fuzzy rule viewer - OCF at B phase

This algorithm can be used to detect and diagnose electrical faults in 5ϕ -PMSM drives with any capacity. To realize this, a 20kW, 5ϕ -PMSM drive [19] was developed, and a performance analysis was conducted. Fig. 44 illustrates the stator current under full load conditions, with a peak value of 37.5 A. Fig. 45 shows the normalized stator current, which has a peak value of 1.34 A and aligns with the performance of the proposed motor. Although the actual peak values of the stator currents differ, their normalized values remain constant across different machine ratings [20]. Since these normalized stator currents are utilized for wavelet analysis, the proposed method can effectively used for the detection and diagnosis of various electrical faults, including ITSF, PPF, PGF, and OCF in 5ϕ -PMSM drives with any capacity.

Table 5	Comparison	table	with	existing	methods

SL No	Fault diagnosis method	Detection time	Types of faults detected				
			Electrical faults				
	memod	unc		SCF		OCF	
			ITSCF	PPF	PGF	OCF	
1	Hilbert Transform method [3]	1 sec	Yes	No	No	No	
2	Self-adapted model predictive current control method [6]	0.8 sec	Yes	Yes	No	Yes	
3	Third-order harmonic back EMF [7]	0.2 sec	Yes	No	No	Yes	
4	Field-oriented control strategy [8]	2 msec	No	No	No	Yes	
5	Magnetic field pendulous oscillation phenomenon [9]	0.6 sec	No	No	No	Yes	
6	Trajectory distribution characteristics of current and terminal voltage [10]	1 sec	No	No	No	Yes	
7	Proposed method	< 0.04 sec	Yes	Yes	Yes	Yes	

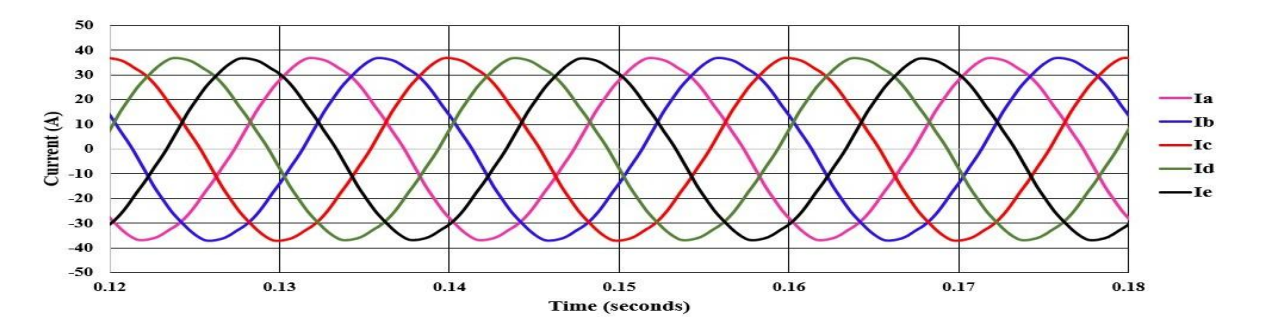


Fig. 44 Stator current at full load condition for $20\,kW$ motor

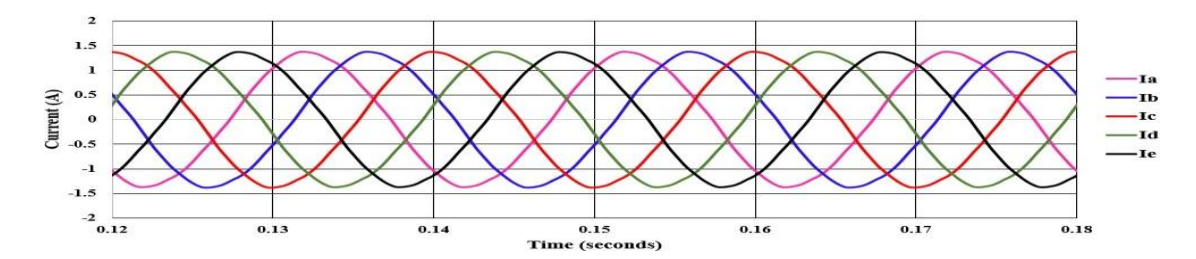


Fig. 45 Normalised stator current at full load condition for 20 kW motor

The novelty of the proposed algorithm is validated by comparing it with the existing fault detection and diagnosis techniques found in the literature, as summarized in Table 5. While the current algorithms are only capable of detecting and diagnosing a single fault at a time, the proposed algorithm can simultaneously detect and diagnose all the electrical faults (ITSF, PPF, PGF, and OCF) within two cycles of the normalized stator currents. A hardware setup is implemented to evaluate the efficacy of the proposed algorithm.

VI. EXPERIMENTAL SETUP

Fig. 46 shows the hardware setup of the proposed diagnosis algorithm, which consists of the following components: 1. Auto-transformer, 2. Two numbers of 3φ Inverters, 3. Microcontroller and driver circuit, 4. a 1kW, 220V, 5φ-PMSM, 5. Cur- rent sensors, 6. Raspberry Pi, 7. Breadboard with LEDs, and 8. LCD. To experimentally validate the proposed algorithm, a Raspberry Pi 4 Model B is set up with the Raspbian operating system using the Raspberry Pi Imager. The fault detection and diagnosis algorithm is implemented in Python. Essential Python libraries, such as pandas, pywt, and scikit-fuzzy, are installed to support data processing and fault diagnosis procedures.

The Raspberry Pi continuously acquires the stator currents of the 5ϕ -PMSM drive via its GPIO pins and a current sensor circuit. These current readings are then processed using a Daubechies 1 wavelet at level 4 from the PyWavelets library. The transformed data is fed into a Mamdani fuzzy logic model, built with the scikit-fuzzy library and user-defined membership functions, to determine the fault condition of the drive based on the processed data. The system displays the result on the Raspberry Pi terminal after comparing the current value acquired by the system to predetermined fault detection criteria.

The implementation of the output of the proposed algorithm uses an LCD screen with designated green and red areas and corresponding LEDs connected to a Raspberry Pi. Python scripts control the LEDs and LCD. A healthy motor status triggers the green LCD box and LED to blink, while a fault triggers the red LCD box and LED. The status of the motor is also displayed on the LCD screen, as depicted in Figure 47.

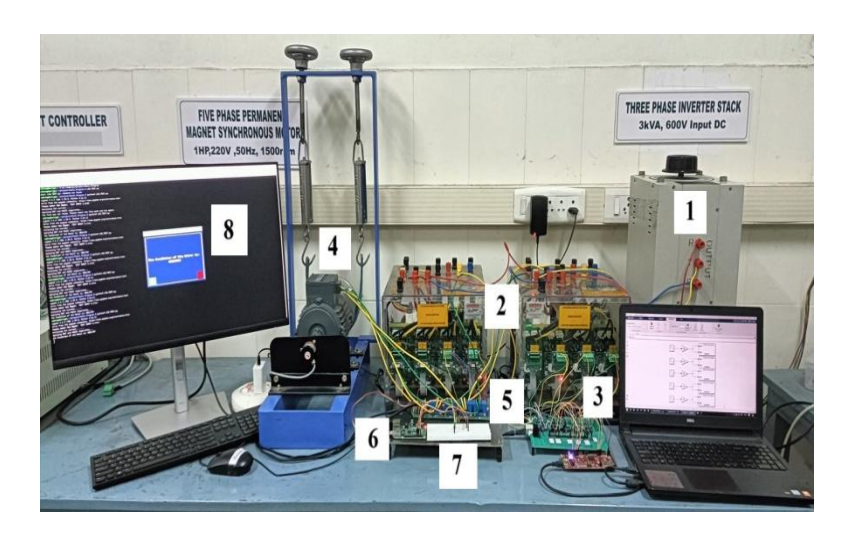


Fig. 46 Experimental setup to validate the fault detection algorithm



Fig. 47 Display system for proposed algorithm

VII. CONCLUSION

The authors developed a single algorithm to detect and diagnose all the electrical faults (ITSF, PPF, PGF, and OCF) in a 5ϕ -PMSM drive. The external editor platform of Ansys Maxwell software is used to develop the model of the motor and the faults. The normalized stator currents of the motor under normal and different electrical faults are analyzed using DWT. The SD of the detailed constants of the db1 wavelet at the 4th level is calculated to identify the faults. A knowledge-based fuzzy logic system is developed to diagnose the faults and the faulty phases. All electrical faults are detected and diagnosed within two cycles of stator currents, which ensures the continuity and reliability of the service. Since the current normalization is considered for DWT analysis, the proposed algorithm can be used to detect and diagnose all electrical faults in the 5ϕ -PMSM drive with any capacity and ratings. The proposed fault detection and diagnosis algorithm is experimentally validated through the Raspberry Pi. The future scope of this work is that it can be used to detect and diagnose other faults, including magnetic, mechanical, and external faults in 5ϕ -PMSM drive.

ACKNOWLEDGEMENT

The authors wish to thank APJ Abdul Kalam Technological University (APJ KTU), and College of Engineering Trivandrum (CET), Kerala, India for supporting this work

REFERENCES

- [1] "Report of Large Motor Reliability Survey of Industrial and Commercial Installations", Part II. IEEE Transactions on Industry Applications, IA-21, pp. 865-872, 1985.
- [2] M. Sabna., Mini V. P, Ushakumari S, Mayadevi N. & Harikumar R, "A Hybrid Fault Detection and Diagnosis Algorithm for Five-Phase PMSM Drive", Arabian Journal for Science and Engineering, pp. 1-13, 2022.
- [3] Jeong H, Lee H, & Kim S. "Inter turn Short Fault Diagnosis Using Magnitude and Phase of Currents in Permanent Magnet Syn-chronous Machines", Advances in Electrical and Computer Engineering, 14, 2022.
- [4] Saavedra H, Riba J R, and Romeral L, "Detection of Inter-turn Faults in Five-Phase Permanent Magnet Synchronous Motors", Advances in Electrical and Computer Engineering, vol.14, no.4, pp.49-54, 2014.

- [5] Wang X, Liu G, Chen Q, Farahat A. & Song X, "Multi vectors Model Predictive Control with Voltage Error Tracking for Five-Phase PMSM Short-Circuit Fault-Tolerant Operation", IEEE Transactions on Transportation Electrification, 8, pp. 675-687, 2022.
- [6] Du Y, Ji J, Zhao W, Tao T. & Xu D, "Self-Adapted Model Predictive Current Control for Five-Phase Open-End Winding PMSM With Reduced Switching Loss", IEEE Transactions on Power Electronics, 37, pp. 11007-11018, 2022.
- [7] Wang H, Gu C, Zhao W, Wang S, Zhang X, Gerada C. & Zhang H, "Fault-Tolerant Control for Single Phase Open-Circuit and Short-Circuit Fault in Five-Phase PMSM with Third-Order Harmonic Back EMF Using Coefficients Reconfiguration", IEEE Transactions On Energy Conversion., 39, pp. 782-792, 2024.
- [8] Xiong C, Guan T, Zhou P & Xu H, "A Fault-Tolerant FOC Strategy for Five- Phase SPMSM With Minimum Torque Ripples in the Full Torque Operation Range Under Double-Phase Open-Circuit Fault", IEEE Transactions on Industrial Electronics, 67, pp. 9059-9072, 2020.
- [9] Chen H, He J, Guan X. & Lee C, "Diagnosis of Open-Phase Faults for a Five-Phase PMSM Fed by a Closed-Loop Vector-Controlled Drive Based on Magnetic Field Pendulous Oscillation Technique", IEEE Transactions On Industrial Electronics, 68, pp. 5582-5593, 2021.
- [10] Tianxing Li, "Diagnosis of open-phase fault of five-phase permanent magnet synchronous motor by harmonic current analysis.", Micro-electronics Reliability, 126, pp. 114205, 2021.
- [11] Sabna M, Mini V. P, S. Ushakumari, Mayadevi N, and Harikumar R, "An Algorithm for Detecting Short Circuit Faults in Five-Phase PMSM Drives," IEEE International Conference on Smart Power Control and Renewable Energy (ICSPCRE), Rourkela, India, pp. 1-6, 2024.
- [12] Kim K, Lim S, Koo D & Lee J, "The Shape Design of Permanent Magnet for Permanent Magnet Synchronous Motor Considering Partial Demagnetization", IEEE Transactions on Magnetics, 42, pp. 3485-3487, 2006.
- [13] Ebrahimi B, Faiz J & Roshtkhari M, "Static-, Dynamic and Mixed-Eccentricity Fault Diagnoses in Permanent-Magnet Synchronous Motors", IEEE Transactions on Industrial Electronics, 56, pp. 4727 4739, 2009.
- [14] Da Y, Shi X & Krishnamurthy M, "A New Approach to Fault Diagnostics for Permanent Magnet Synchronous Machines Using Electromagnetic Signature Analysis", IEEE Transactions on Power Electronics, 28, pp. 4104-4112, 2013.
- [15] Sabna M, Anagha S and Mini V. P, "Design, Modelling, and Performance Comparison of Five-Phase PMSM Drive", International Conference on Electrical Electronics and Computing Technologies (ICEECT), Greater Noida, India, 2024.
- [16] Sabna M, Mini V.P, Ushakumari S, Mayadevi N, Harikumar R. & Vijayasree G, "Inter Turn Short Circuit Fault Analysis of Five-Phase PMSM", IEEE 4th International Conference on Computing, Power And Communication Technologies (GUCON), pp.1-6, 2021.
- [17] Veerendra A, Mohamed M & Punya Sekhar C, "A novel fault-detection methodology of proposed reduced switch MLI fed induction motor drive using discrete wavelet transforms", International Transactions on Electrical Energy Systems., 31, pp.12820, 2021.
- [18] Prosvirin A, Ahmad Z & Kim J, "Global and local feature extraction using a convolutional auto encoder and neural networks for diagnosing centrifugal pump mechanical faults", IEEE Access, 9 pp. 65838-65854, 2021.
- [19] Chen Y & Liu B, "Design and analysis of a five-phase fault-tolerant permanent magnet synchronous motor for aerospace starter generator system", IEEE Access, 7, pp. 135040- 135049,2019.

[20] Kumar H, Pillai R, Nanappan M, Valiyakulam M, Pushpangadan P & Sathyabhama, "A Robust Technique for Detection, Diagnosis, and Localization of Switching Faults in Electric Drives Using Discrete Wavelet Transform", International Journal of Engineering And Technology Innovation, 2023.